Micropumps, microturbines, and flow physics in microdevices

Mohamed Gad-el-Hak

Virginia Commonwealth University, Richmond, VA USA 23284-3015

ABSTRACT

Manufacturing processes that can create extremely small machines have been developed in recent years. Microelectromechanical systems (MEMS) refer to devices that have characteristic length of less than 1 mm but more than 1 micron, that combine electrical and mechanical components and that are fabricated using integrated circuit batch-processing techniques. Electrostatic, magnetic, pneumatic and thermal actuators, motors, valves, gears and tweezers of less than 100 mm size have been fabricated. These have been used as sensors for pressure, temperature, mass flow, velocity and sound, as actuators for linear and angular motions, and as simple components for complex systems such as micro-heat-engines and micro-heat-pumps. The technology is progressing at a rate that far exceeds that of our understanding of the unconventional physics involved in the operation as well as the manufacturing of those minute devices. The primary objective of this paper is to critically review the status of our understanding of fluid flow phenomena particular to microdevices. Continuum as well as molecular approaches to the problem will be surveyed. A second objective is to discuss a novel pump/turbine suited for MEMS applications.

1. INTRODUCTION

Tool making has always differentiated our species from all others on Earth. Aerodynamically correct wooden spears were carved by archaic Homo sapiens close to 400,000 years ago. Man builds things consistent with his size, typically in the range of two orders of magnitude larger or smaller than himself, as indicated in Figure 1. But humans have always striven to explore, build and control the extremes of length and time scales. In the voyages to Lilliput and Brobdingnag of Gulliver s Travels, Jonathan Swift speculated on the remarkable possibilities which diminution or magnification of physical dimensions provides. The Great Pyramid of Khufu was originally 147 m high when completed around 2600 B.C., while the Empire State Building constructed in 1931 is presently after the addition of a television antenna mast in 1950 449 m high. At the other end of the spectrum of man-made artifacts, a dime is slightly less than 2 cm in diameter. Watchmakers have practiced the art of miniaturization since the thirteenth century. The invention of the microscope in the seventeenth century opened the way for direct observation of microbes and plant and animal cells. Smaller things were man-made in the latter half of this century. The transistor invented in 1947 in today integrated circuits has a size of 0.25 micron in production and approaches 50 nanometers in research laboratories. But what about the miniaturization of mechanical parts machines envisioned by Richard Feynman in a legendary lecture delivered in 1959?

Microelectromechanical systems refer to devices that have characteristic length of less than 1 mm but more than 1 micron, that combine electrical and mechanical components and that are fabricated using integrated circuit batch-processing technologies. Current manufacturing techniques for MEMS include surface silicon micromachining; bulk silicon micromachining; lithography, electrodeposition and plastic molding (or, in its original German, Lithographie Galvanoformung Abformung, LIGA); and electrodischarge machining (EDM).

MEMS are finding increased applications in a variety of industrial and medical fields, with a potential worldwide market in the billions of dollars. Accelerometers for automobile airbags, keyless entry systems, dense arrays of micromirrors for high-definition optical displays, scanning electron microscope tips to image single atoms, micro-heat-exchangers for cooling of electronic circuits, reactors for separating biological cells, blood analyzers and pressure sensors for catheter tips are but a few of current usage. Microducts are used in infrared detectors, diode
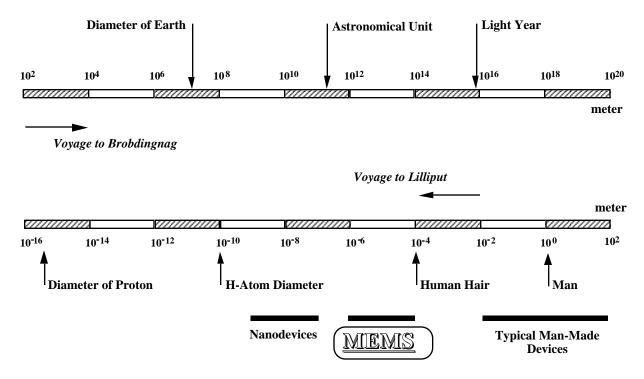
Diameter of Earth   **Astronomical Unit**   **Light Year**

10^2 10^4 10^6 10^8 10^{10} 10^{12} 10^{14} 10^{16} 10^{18} 10^{20}

meter

Voyage to Brobdingnag

Voyage to Lilliput

meter

10^{-16} 10^{-14} 10^{-12} 10^{-10} 10^{-8} 10^{-6} 10^{-4} 10^{-2} 10^{0} 10^{2}

Diameter of Proton   **H-Atom Diameter**   **Human Hair**   **Man**

Nanodevices   MEMS   **Typical Man-Made Devices**

Figure 1. The Scale of things in meter. Lower scale continues in the upper bar from left to right.

lasers, miniature gas chromatographs and high-frequency fluidic control systems. Micropumps are used for ink jet printing, environmental testing and electronic cooling. Potential medical applications for small pumps include controlled delivery and monitoring of minute amount of medication, manufacturing of nanoliters of chemicals and development of artificial pancreas.

Not all MEMS devices involve fluid flows, but the present paper will focus on the ones that do. Microducts, micropumps, microturbines and microvalves are examples of small devices involving the flow of liquids and gases. MEMS can also be related to fluid flows in an indirect way. The availability of inexpensive, batch-processing-produced microsensors and microactuators provides opportunities for targeting small-scale coherent structures in macroscopic turbulent shear flows. Flow control using MEMS promises a quantum leap in control system performance. Because of size limitation, the present paper only touches on its broad subject matter and the reader is referred to three other sources for further details (Gad-el-Hak, 1999; 2000; 2002). The present article is an abridged version of Chapters 4 and 26 of the handbook by Gad-el-Hak (2002).

2. FLUID MECHANICS ISSUES

The rapid progress in fabricating and utilizing microelectromechanical systems during the last decade has not been matched by corresponding advances in our understanding of the unconventional physics involved in the operation and manufacture of small devices. Providing such understanding is crucial to designing, optimizing, fabricating and operating improved MEMS devices.

Fluid flows in small devices differ from those in macroscopic machines. The operation of MEMS-based ducts, nozzles, valves, bearings, turbomachines, etc., cannot always be predicted from conventional flow models such as the Navier—Stokes equations with no-slip boundary condition at a fluid-solid interface, as routinely and successfully applied for larger flow devices. Many questions have been raised when the results of experiments with microdevices could not be explained via traditional flow modeling. The pressure gradient in a long microduct was observed to be non-constant and the measured flowrate was higher than that predicted from the conventional continuum flow model. Load capacities of microbearings were diminished and electric currents needed to move

micromotors were extraordinarily high. The dynamic response of micromachined accelerometers operating at atmospheric conditions was observed to be over-damped.

In the early stages of development of this exciting new field, the objective was to build MEMS devices as productively as possible. Microsensors were reading something, but not many researchers seemed to know exactly what. Microactuators were moving, but conventional modeling could not precisely predict their motion. After a decade of unprecedented progress in MEMS technology, perhaps the time is now ripe to take stock, slow down a bit and answer the many questions that arose. The ultimate aim of this long-term exercise is to achieve rational-design capability for useful microdevices and to be able to characterize definitively and with as little empiricism as possible the operations of microsensors and microactuators.

In dealing with fluid flow through microdevices, one is faced with the question of which model to use, which boundary condition to apply and how to proceed to obtain solutions to the problem at hand. Obviously surface effects dominate in small devices. The surface-to-volume ratio for a machine with a characteristic length of 1 m is 1 m^{-1}, while that for a MEMS device having a size of 1 μm is 10^6 m^{-1}. The million-fold increase in surface area relative to the mass of the minute device substantially affects the transport of mass, momentum and energy through the surface. The small length-scale of microdevices may invalidate the continuum approximation altogether. Slip flow, thermal creep, rarefaction, viscous dissipation, compressibility, intermolecular forces and other unconventional effects may have to be taken into account, preferably using only first principles such as conservation of mass, Newton s second law, conservation of energy, etc.

In this paper, I shall discuss continuum as well as molecular-based flow models, and the choices to be made. Computing typical Reynolds, Mach and Knudsen numbers for the flow through a particular device is a good start to characterize the flow. For gases, microfluid mechanics has been studied by incorporating slip boundary conditions, thermal creep, viscous dissipation as well as compressibility effects into the continuum equations of motion. Molecular-based models have also been attempted for certain ranges of the operating parameters. Use is made of the well-developed kinetic theory of gases, embodied in the Boltzmann equation, and direct simulation methods such as Monte Carlo. Microfluid mechanics of liquids is more complicated. The molecules are much more closely packed at normal pressures and temperatures, and the attractive or cohesive potential between the liquid molecules as well as between the liquid and solid ones plays a dominant role if the characteristic length of the flow is sufficiently small. In cases when the traditional continuum model fails to provide accurate predictions or postdictions, expensive molecular dynamics simulations seem to be the only first-principle approach available to rationally characterize liquid flows in microdevices. Such simulations are not yet feasible for realistic flow extent or number of molecules. As a consequence, the micro-fluid-mechanics of liquids is much less developed than that for gases. The article will conclude with a very brief discussion of a novel pump/turbine suited for MEMS applications.

3. FLUID MODELING

There are basically two ways of modeling a flowfield. Either as the fluid really is a collection of molecules or as a continuum where the matter is assumed continuous and indefinitely divisible. The former modeling is subdivided into deterministic methods and probabilistic ones, while in the latter approach the velocity, density, pressure, etc., are defined at every point in space and time, and conservation of mass, energy and momentum lead to a set of nonlinear partial differential equations (Euler, Navier—Stokes, Burnett, etc.). Fluid modeling classification is depicted schematically in Figure 2.

The continuum model, embodied in the Navier—Stokes equations, is applicable to numerous flow situations. The model ignores the molecular nature of gases and liquids and regards the fluid as a continuous medium describable in terms of the spatial and temporal variations of density, velocity, pressure, temperature and other macroscopic flow quantities. For dilute gas flows near equilibrium, the Navier—Stokes equations are derivable from the molecularly-based Boltzmann equation, but can also be derived independently of that for both liquids and gases. In the case of direct derivation, some empiricism is necessary to close the resulting indeterminate set of equations. The continuum model is easier to handle mathematically (and is also more familiar to most fluid dynamicists)
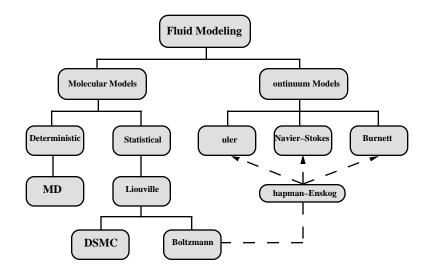
Figure 2. Molecular and continuum flow models.

than the alternative molecular models. Continuum models should therefore be used as long as they are applicable. Thus, careful considerations of the validity of the Navier—Stokes equations and the like are in order

Basically, the continuum model leads to fairly accurate predictions as long as local properties such as density and velocity can be defined as averages over elements large compared with the microscopic structure of the fluid but small enough in comparison with the scale of the macroscopic phenomena to permit the use of differential calculus to describe them. Additionally, the flow must not be too far from thermodynamic equilibrium. The former condition is almost always satisfied, but it is the latter which usually restricts the validity of the continuum equations. As will be seen in the following section, the continuum flow equations do not form a determinate set. The shear stress and heat flux must be expressed in terms of lower-order macroscopic quantities such as velocity and temperature, and the simplest (i.e. linear) relations are valid only when the flow is near thermodynamic equilibrium. Worse yet, the traditional no-slip boundary condition at a solid-fluid interface breaks down even before the linear stress—strain relation becomes invalid.

To be more specific, we temporarily restrict the discussion to gases where the concept of mean free path is well defined. Liquids are more problematic and we defer their discussion to a later section. For gases, the mean free path L is the average distance traveled by molecules between collisions. For an ideal gas modeled as rigid spheres, the mean free path is related to temperature T and pressure p as follows

$$L = \frac{1}{\sqrt{2}\,\pi n\,\sigma^2} = \frac{kT}{\sqrt{2}\,\pi p\,\sigma^2} \tag{1}$$

where n is the number density (number of molecules per unit volume), σ is the molecular diameter, and k is the Boltzmann constant (1.38×10^{-23} J/K.molecule).

The Navier—Stokes equations are valid when L is much smaller than a characteristic flow dimension L. As this condition is violated, the flow is no longer near equilibrium and the linear relation between stress and rate of strain and the no-slip velocity condition are no longer valid. Similarly, the linear relation between heat flux and temperature gradient and the no-jump temperature condition at a solid-fluid interface are no longer accurate when L is not much smaller than L.

The length-scale L can be some overall dimension of the flow, but a more precise choice is the scale of the gradient of a macroscopic quantity, as for example the density ρ,

$$L = \frac{\rho}{\left|\frac{\partial \rho}{\partial y}\right|} \tag{2}$$

The ratio between the mean free path and the characteristic length is known as the Knudsen number

$$Kn = \frac{L}{L} \tag{3}$$

and generally the traditional continuum approach is valid, albeit with modified boundary conditions, as long as $Kn < 0.1$.

There are two more important dimensionless parameters in fluid mechanics, and the Knudsen number can be expressed in terms of those two. The Reynolds number is the ratio of inertial forces to viscous ones

$$Re = \frac{v_o L}{v} \tag{4}$$

where v_o is a characteristic velocity, and v is the kinematic viscosity of the fluid. The Mach number is the ratio of flow velocity to the speed of sound

$$Ma = \frac{v_o}{a_o} \tag{5}$$

The Mach number is a dynamic measure of fluid compressibility and may be considered as the ratio of inertial forces to elastic ones. From the kinetic theory of gases, the mean free path is related to the viscosity as follows

$$v = \frac{\mu}{\rho} = \tfrac{1}{2} L \bar{v}_m \tag{6}$$

where μ is the dynamic viscosity, and $\bar{v}_m$ is the mean molecular speed which is somewhat higher than the sound speed a_o,

$$\bar{v}_m = \sqrt{\frac{8}{\pi \gamma}} \, a_o \tag{7}$$

where γ is the specific heat ratio (i.e. the isentropic exponent). Combining Equations (3)—(7), we reach the required relation

$$Kn = \sqrt{\frac{\pi \gamma}{2}} \, \frac{Ma}{Re} \tag{8}$$

In boundary layers, the relevant length-scale is the shear-layer thickness δ, and for laminar flows

$$\frac{\delta}{L} \sim \frac{1}{\sqrt{Re}} \tag{9}$$

and therefore

$$Kn \sim \frac{Ma}{Re_\delta} \sim \frac{Ma}{\sqrt{Re}} \tag{10}$$

where Re_δ is the Reynolds number based on the freestream velocity v_o and the boundary layer thickness δ, and Re is based on v_o and the streamwise length-scale L.

Rarefied gas flows are in general encountered in flows in small geometries such as MEMS devices and in low-pressure applications such as high-altitude flying and high-vacuum gadgets. The local value of Knudsen number in a particular flow determines the degree of rarefaction and the degree of validity of the continuum model. The different Knudsen number regimes are determined empirically and are therefore only approximate for a particular flow geometry. The pioneering experiments in rarefied gas dynamics were conducted by Knudsen in 1909. In the limit of zero Knudsen number, the transport terms in the continuum momentum and energy equations are negligible and the Navier—Stokes equations then reduce to the inviscid Euler equations. Both heat conduction and viscous diffusion and dissipation are negligible, and the flow is then approximately isentropic (i.e. adiabatic and reversible) from the continuum viewpoint while the equivalent molecular viewpoint is that the velocity distribution function is everywhere of the local equilibrium or Maxwellian form. As Kn increases, rarefaction effects become more important, and eventually the continuum approach breaks down altogether. The different Knudsen number regimes are depicted in Figure 3.

As an example, consider air at standard temperature (T=288 K) and pressure ($p = 1.01 \times 10^5$ N/m^2). A cube one micron on a side contains 2.54×10^7 molecules separated by an average distance of 0.0034 micron. The gas is considered dilute if the ratio of this distance to the molecular diameter exceeds 7, and in the present example this ratio is 9, barely satisfying the dilute gas assumption. The mean free path computed from Equation (1) is L =0.065
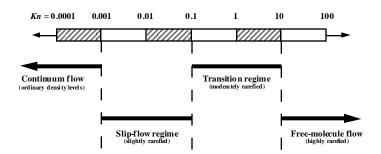
Figure 3. Knudsen number regimes.

μm. A microdevice with characteristic length of 1 μm would have Kn=0.065, which is in the slip-flow regime. At lower pressures, the Knudsen number increases. For example, if the pressure is 0.1 atm and the temperature remains the same, Kn=0.65 for the same 1 μm device, and the flow is then in the transition regime. There would still be over 2 million molecules in the same one-micron cube, and the average distance between them would be 0.0074 μm. The same device at 100 km altitude would have $Kn = 3 \times 10^4$, well into the free-molecule flow regime. Knudsen number for the flow of a light gas like helium is about 3 times larger than that for air flow at otherwise the same conditions.

Consider a long microchannel where the entrance pressure is atmospheric and the exit conditions are near vacuum. As air goes down the duct, the pressure and density decrease while the velocity, Mach number and Knudsen number increase. The pressure drops to overcome viscous forces in the channel. If isothermal conditions prevail, density also drops and conservation of mass requires the flow to accelerate down the constant-area tube. The fluid acceleration in turn affects the pressure gradient, resulting in a nonlinear pressure drop along the channel. The Mach number increases down the tube, limited only by choked-flow condition Ma=1. Additionally, the normal component of velocity is no longer zero. With lower density, the mean free path increases and Kn correspondingly increases. All flow regimes depicted in Figure 3 may occur in the same tube: continuum with no-slip boundary conditions, slip-flow regime, transition regime and free-molecule flow. The air flow may also change from incompressible to compressible as it moves down the microduct. A similar scenario may take place if the entrance pressure is, say, 5 atm, while the exit is atmospheric. This deceivingly simple duct flow may in fact manifest every single complexity discussed in this section. In the following four sections, we discuss in turn the Navier—Stokes equations, compressibility effects, boundary conditions, and molecular-based models.

4. CONTINUUM MODEL

We recall in this section the traditional conservation relations in fluid mechanics. A concise derivation of these equations can be found in Gad-el-Hak (2000). In here, we re-emphasize the precise assumptions needed to obtain a particular form of the equations. A continuum fluid implies that the derivatives of all the dependent variables exist in some reasonable sense. In other words, local properties such as density and velocity are defined as averages over elements large compared with the microscopic structure of the fluid but small enough in comparison with the scale of the macroscopic phenomena to permit the use of differential calculus to describe them. As mentioned earlier, such conditions are almost always met. For such fluids, and assuming the laws of non-relativistic mechanics hold, the conservation of mass, momentum and energy can be expressed at every point in space and time as a set of 5 partial differential equations as for 17 unknowns. Obviously, the continuum flow equations do not form a determinate set. To close the conservation equations, relation between the stress tensor and deformation rate, relation between the heat flux vector and the temperature field and appropriate equations of state relating the different thermodynamic properties are needed. The stress—rateof strain relation and the heat flux—temperature gradient relation are approximately linear if the flow is not too far from thermodynamic equilibrium. This is a phenomenological result but can be rigorously derived from the Boltzmann equation for a dilute gas assuming the flow is near equilibrium. The resulting 6 equations in 6 unknown together with sufficient number of initial and boundary conditions constitute a well-posed, albeit formidable, problem. The system of equations is an excellent

model for the laminar or turbulent flow of most fluids such as air and water under many circumstances, including high-speed gas flows for which the shock waves are thick relative to the mean free path of the molecules.

Considerable simplification is achieved if the flow is assumed incompressible, usually a reasonable assumption provided that the characteristic flow speed is less than 0.3 of the speed of sound. The incompressibility assumption is readily satisfied for almost all liquid flows and many gas flows. In such cases, the density is assumed either a constant or a given function of temperature (or species concentration).

5. COMPRESSIBILITY

The issue of whether to consider the continuum flow compressible or incompressible seems to be rather straightforward, but is in fact full of potential pitfalls. If the local Mach number is less than 0.3, then the flow of a compressible fluid like air can according to the conventional wisdom be treated as incompressible. But the well-known $Ma < 0.3$ criterion is only a necessary not a sufficient one to allow a treatment of the flow as approximately incompressible. In other words, there are situations where the Mach number can be exceedingly small while the flow is compressible. As is well documented in heat transfer textbooks, strong wall heating or cooling may cause the density to change sufficiently and the incompressible approximation to break down, even at low speeds. Less known is the situation encountered in some microdevices where the pressure may strongly change due to viscous effects even though the speeds may not be high enough for the Mach number to go above the traditional threshold of 0.3. Corresponding to the pressure changes would be strong density changes that must be taken into account when writing the continuum equations of motion.

Experiments in gaseous microducts confirm the above arguments. For both low- and high-Mach-number flows, pressure gradients in long microchannels are non-constant, consistent with the compressible flow equations. There are three additional scenarios in which significant pressure and density changes may take place without inertial, viscous or thermal effects. First is the case of quasi-static compression/expansion of a gas in, for example, a piston-cylinder arrangement. The resulting compressibility effects are, however, compressibility of the fluid and not of the flow. Two other situations where compressibility effects must also be considered are problems with length-scales comparable to the scale height of the atmosphere and rapidly varying flows as in sound propagation.

6. BOUNDARY CONDITIONS

The continuum equations of motion described earlier require a certain number of initial and boundary conditions for proper mathematical formulation of flow problems. In this section, we describe the boundary conditions at a fluid-solid interface. Boundary conditions in the inviscid flow theory pertain only to the velocity component normal to a solid surface. The highest spatial derivative of velocity in the inviscid equations of motion is first-order, and only one velocity boundary condition at the surface is admissible. The normal velocity component at a fluid-solid interface is specified, and no statement can be made regarding the tangential velocity component. The normal-velocity condition simply states that a fluid-particle path cannot go through an impermeable wall. Real fluids are of course viscous and the corresponding momentum equation has second-order derivatives of velocity, thus requiring an additional boundary condition on the velocity component tangential to a solid surface.

Traditionally, the no-slip condition at a fluid-solid interface is enforced in the momentum equation and an analogous no-temperature-jump condition is applied in the energy equation. The notion underlying the no-slip/no-jump condition is that within the fluid there cannot be any finite discontinuities of velocity/temperature. Those would involve infinite velocity/temperature gradients and so produce infinite viscous stress/heat flux that would destroy the discontinuity in infinitesimal time. The interaction between a fluid particle and a wall is similar to that between neighboring fluid particles, and therefore no discontinuities are allowed at the fluid-solid interface either. In other words, the fluid velocity must be zero relative to the surface and the fluid temperature must equal to that of the surface. But strictly speaking those two boundary conditions are valid only if the fluid flow adjacent to the surface is in thermodynamic equilibrium. This requires an infinitely high frequency of collisions between the fluid and the solid surface. In practice, the no-slip/no-jump condition leads to fairly accurate predictions as long as $Kn < 0.001$ (for gases). Beyond that, the collision frequency is simply not high enough to ensure equilibrium and a certain degree of tangential-velocity slip and temperature jump must be allowed. This is a case frequently encountered in MEMS flows, and we develop the appropriate relations in this section.

Assuming isothermal conditions prevail, the above slip relation has been rigorously derived by Maxwell (1879) from considerations of the kinetic theory of dilute, monatomic gases. Gas molecules, modeled as rigid spheres, continuously strike and reflect from a solid surface, just as they continuously collide with each other. For an idealized perfectly smooth wall (at the molecular scale), the incident angle exactly equals the reflected angle and the molecules conserve their tangential momentum and thus exert no shear on the wall. This is termed specular reflection and results in perfect slip at the wall. For an extremely rough wall, on the other hand, the molecules reflect at some random angle uncorrelated with their entry angle. This perfectly diffuse reflection results in zero tangential-momentum for the reflected fluid molecules to be balanced by a finite slip velocity in order to account for the shear stress transmitted to the wall. A force balance near the wall leads to the following expression for the slip velocity

$$u_{gas} - u_{wall} = L \left. \frac{\partial u}{\partial y} \right|_w \tag{11}$$

where L is the mean free path. The right-hand side can be considered as the first term in an infinite Taylor series, sufficient if the mean free path is relatively small enough. The equation above states that significant slip occurs only if the mean velocity of the molecules varies appreciably over a distance of one mean free path. This is the case, for example, in vacuum applications and/or flow in microdevices. The number of collisions between the fluid molecules and the solid in those cases is not large enough for even an approximate flow equilibrium to be established. Furthermore, additional (nonlinear) terms in the Taylor series would be needed as L increases and the flow is further removed from the equilibrium state.

For real walls some molecules reflect diffusively and some reflect specularly. In other words, a portion of the momentum of the incident molecules is lost to the wall and a (typically smaller) portion is retained by the reflected molecules. The tangential-momentum-accommodation coefficient σ_v is defined as the fraction of molecules reflected diffusively. This coefficient depends on the fluid, the solid and the surface finish, and has been determined experimentally to be between 0.2—0.8, the lower limit being for exceptionally smooth surfaces while the upper limit is typical of most practical surfaces. The final expression derived by Maxwell for an isothermal wall reads

$$u_{gas} - u_{wall} = \frac{2 - \sigma_v}{\sigma_v} L \left. \frac{\partial u}{\partial y} \right|_w \tag{12}$$

For $\sigma_v = 0$, the slip velocity is unbounded, while for $\sigma_v = 1$, Equation (12) reverts to (11). Similar arguments were made for the temperature-jump boundary condition by von Smoluchowski (1898).

7. MOLECULAR-BASED MODELS

In the continuum models discussed thus far, the macroscopic fluid properties are the dependent variables while the independent variables are the three spatial coordinates and time. The molecular models recognize the fluid as a myriad of discrete particles: molecules, atoms, ions and electrons. The goal here is to determine the position, velocity and state of all particles at all times. The molecular approach is either deterministic or probabilistic (refer to Figure 2). Provided that there is a sufficient number of microscopic particles within the smallest significant volume of a flow, the macroscopic properties at any location in the flow can then be computed from the discrete-particle information by a suitable averaging or weighted averaging process. The present section discusses molecular-based models and their relation to the continuum models previously considered.

The most fundamental of the molecular models is a deterministic one. The motion of the molecules are governed by the laws of classical mechanics, although, at the expense of greatly complicating the problem, the laws of quantum mechanics can also be considered in special circumstances. The modern molecular dynamics computer simulations (MD) have been pioneered by Alder and Wainwright (1957; 1958; 1970) and reviewed by Ciccotti and Hoover (1986), Allen and Tildesley (1987), Haile (1993) and Koplik and Banavar (1995). The simulation begins with a set of N molecules in a region of space, each assigned a random velocity corresponding to a Boltzmann distribution at the temperature of interest. The interaction between the particles is prescribed typically in the form of a two-body potential energy and the time evolution of the molecular positions is determined by integrating Newton s equations of motion. Because MD is based on the most basic set of equations, it is valid in principle for any flow extent and any range of parameters. The method is straightforward in principle but there are two hurdles: choosing a proper and convenient potential for particular fluid and solid combinations, and the colossal computer resources required to simulate a reasonable flowfield extent.

For purists, the former difficulty is a sticky one. There is no totally rational methodology by which a convenient potential can be chosen. Part of the art of MD is to pick an appropriate potential and validate the simulation results with experiments or other analytical/computational results. A commonly used potential between two molecules is the generalized Lennard-Jones 6—12 potential, to be used in the following section and further discussed in the section following that.

The second difficulty, and by far the most serious limitation of molecular dynamics simulations, is the number of molecules N that can realistically be modeled on a digital computer. Since the computation of an element of trajectory for any particular molecule requires consideration of *all* other molecules as potential collision partners, the amount of computation required by the MD method is proportional to N^2. Some saving in computer time can be achieved by cutting off the weak tail of the potential at, say, $r_c = 2.5\sigma$, and shifting the potential by a linear term in r so that the force goes smoothly to zero at the cutoff. As a result, only nearby molecules are treated as potential collision partners, and the computation time for N molecules no longer scales with N^2.

The state of the art of molecular dynamics simulations in the early 2000s is such that with a few hours of CPU time, general purpose supercomputers can handle around 100,000 molecules. At enormous expense, the fastest parallel machine available can simulate around 10 million particles. Because of the extreme diminution of molecular scales, the above translates into regions of liquid flow of about 0.02 μm (200 Angstroms) in linear size, over time intervals of around 0.001 μs, enough for continuum behavior to set in for simple molecules. To simulate 1 s of real time for complex molecular interactions, e.g. including vibration modes, reorientation of polymer molecules, collision of colloidal particles, etc., requires unrealistic CPU time measured in hundreds of years.

MD simulations are highly inefficient for dilute gases where the molecular interactions are infrequent. The simulations are more suited for dense gases and liquids. Clearly, molecular dynamics simulations are reserved for situations where the continuum approach or the statistical methods are inadequate to compute from first principles important flow quantities. Slip boundary conditions for liquid flows in extremely small devices is such a case as will be discussed in the following section.

An alternative to the deterministic molecular dynamics is the statistical approach where the goal is to compute the probability of finding a molecule at a particular position and state. If the appropriate conservation equation can be solved for the probability distribution, important statistical properties such as the mean number, momentum or energy of the molecules within an element of volume can be computed from a simple weighted averaging. In a practical problem, it is such average quantities that concern us rather than the detail for every single molecule. Clearly, however, the accuracy of computing average quantities, via the statistical approach, improves as the number of molecules in the sampled volume increases. The kinetic theory of dilute gases is well advanced, but that for dense gases and liquids is much less so due to the extreme complexity of having to include multiple collisions and intermolecular forces in the theoretical formulation.

In the statistical approach, the fraction of molecules in a given location and state is the sole dependent variable. The independent variables for monatomic molecules are time, the three spatial coordinates and the three components of molecular velocity. Those describe a 6-dimensional phase space. For diatomic or polyatomic molecules, the dimension of phase space is increased by the number of internal degrees of freedom. Orientation adds an extra dimension for molecules which are not spherically symmetric. Finally, for mixtures of gases, separate probability distribution functions are required for each species. Clearly, the complexity of the approach increases dramatically as the dimension of phase space increases. The simplest problems are, for example, those for steady, one-dimensional flow of a simple monatomic gas.

To simplify the problem we restrict the discussion here to monatomic gases having no internal degrees of freedom. Furthermore, the fluid is restricted to dilute gases and molecular chaos is assumed. The former restriction requires the average distance between molecules δ to be an order of magnitude larger than their diameter σ. That will almost guarantee that all collisions between molecules are binary collisions, avoiding the complexity of modeling multiple encounters. The molecular chaos restriction improves the accuracy of computing the macroscopic quantities from the microscopic information. In essence, the volume over which averages are computed has to have sufficient number of molecules to reduce statistical errors. It can be shown that computing macroscopic flow

properties by averaging over a number of molecules will result in statistical fluctuations with a standard deviation of approximately 0.1% if one million molecules are used and around 3% if one thousand molecules are used. The molecular chaos limit requires the length-scale L for the averaging process to be at least 100 times the average distance between molecules (i.e. typical averaging over at least one million molecules).
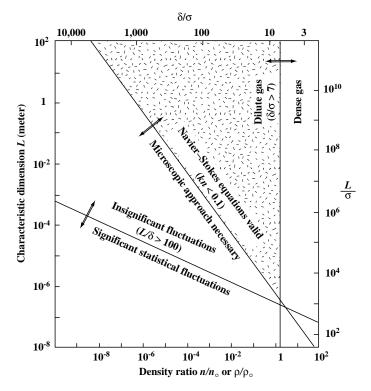

Figure 4. Effective limits of different flow models.

Figure 4, adapted from Bird (1994), shows the limits of validity of the dilute gas approximation ($\delta/\sigma > 7$), the continuum approach ($Kn < 0.1$, as discussed previously), and the neglect of statistical fluctuations ($L/\delta > 100$). Using a molecular diameter of $\sigma = 4 \times 10^{-10}$ m as an example, the three limits are conveniently expressed as functions of the normalized gas density ρ/ρ_o or number density n/n_o, where the reference densities ρ_o and n_o are computed at standard conditions. All three limits are straight lines in the log-log plot of L versus ρ/ρ_o, as depicted in Figure 4. Note the shaded triangular wedge inside which both the Boltzmann and Navier—Stokes equations are valid. Additionally, the lines describing the three limits very nearly intersect at a single point. As a consequence, the continuum breakdown limit always lies between the dilute gas limit and the limit for molecular chaos. As density or characteristic dimension is reduced in a dilute gas, the Navier—Stokes model breaks down before the level of statistical fluctuations becomes significant. In a dense gas, on the other hand, significant fluctuations may be present even when the Navier—Stokes model is still valid.

8. MICROPUMPS

There have been several studies of microfabricated pumps. Some of them use non-mechanical effects. The Knudsen pump uses the thermal-creep effect to move rarefied gases from one chamber to another. Ion-drag is used in electrohydrodynamic pumps (Bart et al., 1990; Richter et al., 1991; Fuhr et al., 1992); these rely on the electrical properties of the fluid and are thus not suitable for many applications. Valveless pumping by ultrasound has also been proposed (Moroney et al., 1991), but produces very little pressure difference.

Mechanical pumps based on conventional centrifugal or axial turbomachinery will not work at micromachine scales where the Reynolds numbers are typically small, on the order of 1 or less. Centrifugal forces are negligible and, furthermore, the Kutta condition through which lift is normally generated is invalid when inertial forces are vanishingly small. In general there are three ways in which mechanical micropumps can work:

- Positive-displacement pumps. These are mechanical pumps with a membrane or diaphragm actuated in a reciprocating mode and with unidirectional inlet and outlet valves. They work on the same physical principle as their larger cousins. Micropumps with piezoelectric actuators have been fabricated (Van Lintel et al., 1988; Esashi et al., 1989; Smits, 1990). Other actuators, such as thermopneumatic, electrostatic, electromagnetic or bimetallic, can be used (Pister et al., 1990; Döring et al., 1992; Gabriel et al., 1992). These exceedingly minute positive-displacement pumps require even smaller valves, seals and mechanisms, a not-too-trivial micromanufacturing challenge. In addition there are long-term problems associated with wear or clogging and consequent leaking around valves. The pumping capacity of these pumps is also limited by the small displacement and frequency involved. Gear pumps are a different kind of positive-displacement device.

- Continuous, parallel-axis rotary pumps. A screw-type, three-dimensional device for low Reynolds numbers was proposed by Taylor (1972) for propulsion purposes and shown in his seminal film. It has an axis of rotation parallel to the flow direction implying that the powering motor must be submerged in the flow, the flow turned through an angle, or that complicated gearing would be needed.

- Continuous, transverse-axis rotary pumps. This is the class of machines that was recently developed by Sen et al. (1996). They have shown that a rotating body, asymmetrically placed within a duct, will produce a net flow due to viscous action. The axis of rotation can be perpendicular to the flow direction and the cylinder can thus be easily powered from outside a duct. A related viscous-flow pump was designed by Odell and Kovasznay (1971) for a water channel with density stratification. However, their design operates at a much higher Reynolds number and is too complicated for microfabrication.

As evidenced from the third item above, it is possible to generate axial fluid motion in open channels through the rotation of a cylinder in a viscous fluid medium. Odell and Kovasznay (1971) studied a pump based on this principle at high Reynolds numbers. Sen et al. (1996) carried out an experimental study of a different version of such a pump. The novel viscous pump, shown schematically in Figure 5, consists simply of a transverse-axis cylindrical rotor eccentrically placed in a channel, so that the differential viscous resistance between the small and large gaps causes a net flow along the duct.
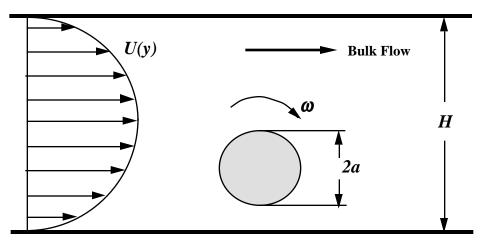

Figure 5. Schematic of micropump developed by Sen et al. (1996).

The Reynolds numbers involved in Sen et al.'s work were low ($0.01 < Re \equiv 2\omega a^2/\upsilon < 10$), where ω is the radian velocity of the rotor, a is its radius, and υ is the fluid kinematic viscosity), typical of microscale devices, but achieved using a macroscale rotor and a very viscous fluid. The bulk velocities obtained were as high as 10% of the surface speed of the rotating cylinder. Sen et al. (1996) have also tried cylinders with square and rectangular cross-sections, but the circular cylinder delivered the best pumping performance.

A finite-element solution for low-Reynolds-number, uniform flow past a rotating cylinder near an impermeable plane boundary has already been obtained by Liang and Liou (1995). However a detailed two-dimensional Navier–Stokes simulations of the pump described above have been carried out by Sharatchandra et al. (1997), who extended the operating range of Re beyond 100. The effects of varying the channel height H and the rotor eccentricity ε have been studied. It was demonstrated that an optimum plate spacing exists and that the induced flow increases monotonically with eccentricity; the maximum flowrate being achieved with the rotor in contact with a channel wall. Both the experimental results of Sen et al. (1996) and the 2-D numerical simulations of Sharatchandra et al. (1997) have verified that, at $Re<10$, the pump characteristics are linear and therefore kinematically reversible. Sharatchandra et al. (1997; 1998a) also investigated the effects of slip flow on the pump performance as well as the thermal aspects of the viscous device. Wall slip does reduce the traction at the rotor surface and thus lowers the performance of the pump somewhat. However, the slip effects appear to be significant only for Knudsen numbers greater than 0.1, which is encouraging from the point of view of microscale applications.

In an actual implementation of the micropump, several practical obstacles need to be considered. Among those are the larger stiction and seal design associated with rotational motion of microscale devices. Both the rotor and the channel have a finite, in fact rather small, width. DeCourtye et al. (1998) numerically investigated the viscous micropump performance as the width of the channel W becomes exceedingly small. The bulk flow generated by the pump decreased as a result of the additional resistance to the flow caused by the side walls. However, effective pumping was still observed with extremely narrow channels. Finally, Shartchandra et al. (1998b) used a genetic algorithm to determine the optimum wall shape to maximize the micropump performance. Their genetic algorithm uncovered shapes that were nonintuitive but yielded vastly superior pump performance.

Though most of the micropump discussion above is of flow in the steady state, it should be possible to give the eccentric cylinder a finite number of turns or even a portion of a turn to displace a prescribed minute volume of fluid. Numerical computations will easily show the order of magnitude of the volume discharged and the errors induced by acceleration at the beginning of the rotation and deceleration at the end. Such system can be used for microdosage delivery in medical applications.

9. MICROTURBINES

DeCourtye et al. (1998) have described the possible utilization of the inverse micropump device as a turbine. The most interesting application of such a microturbine would be as a microsensor for measuring exceedingly small flowrates on the order of nanoliter/s (i.e., microflow metering for medical and other applications).

The viscous pump described in Section 8 operates best at low Reynolds numbers and should therefore be kinematically reversible in the creeping-flow regime. A microturbine based on the same principle should, therefore, lead to a net torque in the presence of a prescribed bulk velocity. The results of three-dimensional numerical simulations of the envisioned microturbine are summarized in this section. The Reynolds number for the turbine problem is defined in terms of the bulk velocity, since the rotor surface speed is unknown in this case, $Re \equiv \overline{U}(2a)/\upsilon$, where $\overline{U}$ is the prescribed bulk velocity in the channel.

The turbine characteristics are defined by the relation between the shaft speed and the applied load. A turbine load results in a moment on the shaft, which at steady state balances the torque due to viscous stresses. At a fixed bulk velocity, the rotor speed is determined for different loads on the turbine. Again, the turbine characteristics are linear in the Stokes (creeping) flow regime, but the side walls have weaker, though still adverse, effect on the device

performance as compared to the pump case. For a given bulk velocity, the rotor speed drops linearly as the external load on the turbine increases. At large enough loads, the rotor will not spin, and maximum rotation is achieved when the turbine is subjected to zero load.

At present it is difficult to measure flowrates on the order of 10^{-12} m^3/s (1 nanoliter/s). One possible way is to directly collect the effluent over time. This is useful for calibration but is not practical for on-line flow measurement. Another is to use heat transfer from a wire or film to determine the local flowrate as in a thermal anemometer. Heat transfer from slowly moving fluids is mainly by conduction so that temperature gradients can be large. This is undesirable for biological and other fluids easily damaged by heat. The viscous mechanism that has been proposed and verified for pumping herein may be turned around and used for measuring. As demonstrated in this section, a freely rotating cylinder eccentrically placed in a duct will rotate at a rate proportional to the flowrate due to a turbine effect. In fact other geometries such as a freely rotating sphere in a cylindrical tube should also behave similarly. The calibration constant, which depends on system parameters such as geometry and bearing friction, should be determined computationally to ascertain the practical viability of such a microflow meter. Geometries that are simplest to fabricate should be explored and studied in detail.

10. MICROBEARINGS

Many of the micromachines use rotating shafts and other moving parts which carry a load and need fluid bearings for support, most of them operating with air or water as the lubricating fluid. The fluid mechanics of these bearings are very different compared to that of their larger cousins. Their study falls in the area of microfluid mechanics, an emerging discipline which has been greatly stimulated by its applications to micromachines and which is the subject of this paper.

Macroscale journal bearings develop their load-bearing capacity from large pressure differences which are a consequence of the presence of a viscous fluid, an eccentricity between the shaft and its housing, a large surface speed of the shaft, and a small clearance to diameter ratio. Several closed-form solutions of the no-slip flow in a macrobearing have been developed. Wannier (1950) used modified Cartesian coordinates to find an exact solution to the biharmonic equation governing two-dimensional journal bearings in the no-slip, creeping flow regime. Kamal (1966) and Ashino and Yoshida (1975) worked in bipolar coordinates; they assumed a general form for the streamfunction with several constants that were determined using the boundary conditions. Though all these methods work if there is no slip, they cannot be readily adapted to slip flow. The basic reason is that the flow pattern changes if there is slip at the walls and the assumed form of the solution is no longer valid.

Microbearings are different in the following aspects: (1) being so small, it is difficult to manufacture them with a clearance that is much smaller than the diameter of the shaft; (2) because of the small shaft size, its surface speed, at normal rotational speeds, is also small; and (3) air bearings in particular may be small enough for non-continuum effects to become important. For these reasons the hydrodynamics of lubrication is very different at microscales. The lubrication approximation that is normally used is no longer directly applicable and other effects come into play. From an analytical point of view there are three consequences of the above: fluid inertia is negligible, slip flow may be important for air and other gases, and relative shaft clearance need not be small.

In a recent study, Maureau et al. (1997) analyzed microbearings represented as an eccentric cylinder rotating in a stationary housing. The flow Reynolds number is assumed small, the clearance between shaft and housing is not small relative to the overall bearing dimensions, and there is slip at the walls due to non-equilibrium effects. The two-dimensional governing equations are written in terms of the streamfunction in bipolar coordinates. Following the method of Jeffery (1920), Maureau et al. (1997) succeeded in obtaining an exact infinite-series solution of the Navier–Stokes equations for the specified geometry and flow conditions. In contrast to macrobearings and due to the large clearance, flow in a microbearing is characterized by the possibility of a recirculation zone which strongly affects the velocity and pressure fields. For high values of the eccentricity and low slip factors the flow develop a recirculation region.

From the infinite-series solution the frictional torque and the load-bearing capacity can be determined. The results show that both are similarly affected by the eccentricity and the slip factor: they increase with the former and decrease with the latter. For a given load, there is a corresponding eccentricity which generates a force sufficient to separate shaft from housing (i.e. sufficient to prevent solid-to-solid contact). As the load changes the rotational center of the shaft shifts a distance necessary for the forces to balance. It is interesting to note that for a weight that is vertically downwards, the equilibrium displacement of the center of the shaft is in the horizontal direction. This can lead to complicated rotor dynamics governed by mechanical inertia, viscous damping and pressure forces. A study of this dynamics may of interest. Real microbearings have finite shaft lengths, and end walls and other three-dimensional effects influence the bearing characteristics. Numerical simulations of the three-dimensional problem can readily be carried out and may also be of interest to the designers of microbearings. Other potential research includes determination of a criterion for onset of cavitation in liquid bearings. From the results of these studies, information related to load, rotational speed and geometry can be generated that would be useful for the designer.

Finally, Piekos et al. (1997) have used full Navier–Stokes computations to study the stability of ultra-high-speed, gas microbearings. They conclude that it is possible—despite significant design constraints—to attain stability for specific bearings to be used with the MIT microturbomachines (Epstein and Senturia, 1997; Epstein et al., 1997), which incidentally operate at much higher Reynolds numbers (and rpm) than the micropumps/microturbines/microbearings considered thus far in this and the previous two sections. According to Piekos et al. (1997), high-speed bearings are more robust than low-speed ones due to their reduced running eccentricities and the large loads required to maintain them.

11. SUMMARY

The traditional Navier—Stokes model of fluid flows with no-slip boundary conditions works only for a certain range of the governing parameters. This model basically demands two conditions. (1) The fluid is a continuum, which is almost always satisfied as there are usually more than one million molecules in the smallest volume in which appreciable macroscopic changes take place. This is the molecular chaos restriction. (2) The flow is not too far from thermodynamic equilibrium, which is satisfied if there is sufficient number of molecular encounters during a time period small compared to the smallest time-scale for flow changes. During this time period the average molecule would have moved a distance small compared to the smallest flow length-scale.

For gases, the Knudsen number determines the degree of rarefaction and the applicability of traditional flow models. As Kn tends to zero, the time- and length-scales of molecular encounters are vanishingly small compared to those for the flow, and the velocity distribution of each element of the fluid instantaneously adjusts to the equilibrium thermodynamic state appropriate to the local macroscopic properties as this molecule moves through the flow field. From the continuum viewpoint, the flow is isentropic and heat conduction and viscous diffusion and dissipation vanish from the continuum conservation relations, leading to the Euler equations of motion. At small but finite Kn, the Navier—Stokes equations describe near-equilibrium, continuum flows.

Gaseous flows are often compressible in microdevices even at low Mach numbers. Viscous effects can cause sufficient pressure drop and density changes for the flow to be treated as compressible. In a long, constant-area microduct, all Knudsen number regimes may be encountered and the degree of rarefaction increases along the tube. The pressure drop is nonlinear and the Mach number increases downstream, limited only by choked-flow condition.

Similar deviation and breakdown of the traditional Navier—Stokes equations occur for liquids as well, but there the situation is more murky. Existing experiments are contradictory. There is no kinetic theory of liquids, and first-principles prediction methods are scarce. Molecular dynamics simulations can be used, but they are limited to extremely small flow extents.

On the application front, simple, viscous-based micropumps can be utilized for microdosage delivery, and microturbines can be used for measuring flowrates in the nanoliter/s range. Both of these can be of value in several medical applications.

The material presented herein is but a very brief summary of a very broad area of research. The reader is referred to the books by Gad-el-Hak (2002) and Karniadakis and Beskok (2002) to fill much of the missing details.

REFERENCES

Alder, B.J., and Wainwright, T.E. (1957) Studies in Molecular Dynamics, *J. Chemical Phys.* **27**, pp. 1208—1209.

Alder, B.J., and Wainwright, T.E. (1958) Molecular Dynamics by Electronic Computers, in *Transport Processes in Statistical Mechanics*, ed. I. Prigogine, pp. 97—131, Interscience, New York.

Alder, B.J., and Wainwright, T.E. (1970) Decay of the Velocity Auto-Correlation Function, *Phy. Rev. A* **1**, pp. 18—21.

Allen, M.P., and Tildesley, D.J. (1987) *Computer Simulation of Liquids*, Clarendon Press, Oxford, Great Britain.

Ashino, I., and Yoshida, K. (1975) Slow Motion between Eccentric Rotating Cylinders, *Bulletin JSME* **18**, no. 117, pp. 280—285.

Bart, S.F., Tavrow, L.S., Mehregany, M., and Lang, J.H. (1990) Microfabricated Electrohydrodynamic Pumps, *Sensors & Actuators A* **21—23**, pp. 193—197.

Bird, G.A. (1994) *Molecular Gas Dynamics and the Direct Simulation of Gas Flows*, Clarendon Press, Oxford, Great Britain.

Ciccotti, G., and Hoover, W.G., editors (1986) *Molecular Dynamics Simulation of Statistical Mechanics Systems*, North Holland, Amsterdam, the Netherlands.

DeCourtye, D., Sen, M., and Gad-el-Hak, M. (1998) Analysis of Viscous Micropumps and Microturbines, *Int. J. Computat. Fluid Dyn*. **10**, pp. 13—25.

Döring, C., Grauer, T., Marek, J., Mettner, M.S., Trah, H.-P., and Willmann, M. (1992) Micromachined Thermoelectrically Driven Cantilever Structures for Fluid Jet Deflection,'' in *Proc. IEEE Micro Electro Mechanical Systems 92*, pp. 12—18, 4—7 February, Travemünde, Germany.

Epstein, A.H., and Senturia, S.D. (1997) Macro Power from Micro Machinery, *Science* **276**, 23 May, p. 1211.

Epstein, A.H., Senturia, S.D., Al-Midani, O., Anathasuresh, G., Ayon, A., Breuer, K., Chen, K.-S., Ehrich, F.F., Esteve, E., Frechette, L., Gauba, G., Ghodssi, R., Groshenry, C., Jacobson, S.A., Kerrebrock, J.L., Lang, J.H., Lin, C.-C., London, A., Lopata, J., Mehra, A., Mur Miranda, J.O., Nagle, S., Orr, D.J., Piekos, E., Schmidt, M.A., Shirley, G., Spearing, S.M., Tan, C.S., Tzeng, Y.-S., and Waitz, I.A. (1997) Micro-Heat Engines, Gas Turbines, and Rocket Engines — The MIT Microengine Project, AIAA Paper No. 97-1773, AIAA, Reston, Virginia.

Esashi, M., Shoji, S., and Nakano, A. (1989) Normally Closed Microvalve Fabricated on a Silicon Wafer, *Sensors & Actuators* **20**, pp. 163—169.

Fuhr, G., Hagedorn, R., Müller, T., Benecke, W., and Wagner, B. (1992) Microfabricated Electrohydrodynamic (EHD) Pumps for Liquids of Higher Conductivity, *J. MEMS* **1**, pp. 141—145.

Gabriel, K.J., Tabata, O., Shimaoka, K., Sugiyama, S., and Fujita, H. (1992) Surface-Normal Electrostatic/Pneumatic Actuator, in *Proc. IEEE Micro Electro Mechanical Systems 92*, pp. 128—131, 4—7 February, Travemünde, Germany.

Gad-el-Hak, M. (1999) The Fluid Mechanics of Microdevices — The Freeman Scholar Lecture, *J. Fluids Eng.* **121**, pp. 5—33.

Gad-el-Hak, M. (2000) *Flow Control: Passive, Active, and Reactive Flow Management*, Cambridge University Press, London, Great Britain.

Gad-el-Hak, M. (2002) *The MEMS Handbook*, CRC Press, Boca Raton, Florida.

Haile, J.M. (1993) *Molecular Dynamics Simulation: Elementary Methods*, Wiley, New York.

Jeffery, G.B. (1920) Plane Stress and Plane Strain in Bipolar Co-ordinates, *Phil. Trans. R. Soc. Ser. A* **221**, pp. 265—289.

Kamal, M.M. (1966) Separation in the Flow Between Eccentric Rotating Cylinders, *Trans. ASME Ser. D* **88**, pp. 717—724.

Karniadakis, G.Em, and Beskok, A. (2002) *Microflows: Fundamentals and Simulation*, Springer-Verlag, New York

Koplik, J., and Banavar, J.R . (1995) Continuum Deductions from Molecular Hydroynamics, *Annu. Rev. Fluid Mech.* **27**, pp. 257—292.

Liang, W.J., and Liou, J.A. (1995) Flow Around a Rotating Cylinder Near a Plane Boundary, *J. Chinese Institute of Engineers* **18**, pp. 35—50.

Maureau, J., Sharatchandra, M.C., Sen, M., and Gad-el-Hak, M. (1997) Flow and Load Characteristics of Microbearings with Slip, *J. Micromech. Microeng.* **7**, pp. 55—64.

Maxwell, J.C. (1879) On Stresses in Rarefied Gases Arising from Inequalities of Temperature, *Phil. Trans. R. Soc. Part 1* **170**, pp. 231—256.

Moroney, R.M., White, R.M., and Howe, R.T. (1991) Ultrasonically Induced Microtransport,'' in *Proc. IEEE Micro Electro Mechanical Systems 91*, pp. 277—282, Nara, Japan, IEEE, New York.

Odell, G.M., and Kovasznay, L.S.G. (1971) A New Type of Water Channel with Density Stratification, *J. Fluid Mech.* **50**, pp. 535—543.

Piekos, E.S., Orr, D.J., Jacobson, S.A., Ehrich, F.F., and Breuer, K.S. (1997) Design and Analysis of Microfabricated High Speed Gas Journal Bearings, AIAA Paper No. 97-1966, AIAA, Reston, Virginia.

Pister, K.S.J., Fearing, R.S., and Howe, R.T. (1990) A Planar Air Levitated Electrostatic Actuator System, IEEE Paper No. CH2832-4/90/0000-0067, IEEE, New York.

Richter, A., Plettner, A., Hofmann, K.A., and Sandmaier, H. (1991) A Micromachined Electrohydrodynamic (EHD) Pump, *Sensors & Actuators A* **29**, pp. 159—168.

Sen, M., Wajerski, D., and Gad-el-Hak, M. (1996) A Novel Pump for MEMS Applications, *J. Fluids Eng.* **118**, pp. 624—627.

Sharatchandra, M.C., Sen, M., and Gad-el-Hak, M. (1997) Navier—Stokes Simulations of a Novel Viscous Pump, *J. Fluids Eng.* **119**, pp. 372—382.

Sharatchandra, M.C., Sen, M., and Gad-el-Hak, M. (1998a) Thermal Aspects of a Novel Micropumping Device, *J. Heat Transfer* **120**, pp. 99—107.

Sharatchandra, M.C., Sen, M., and Gad-el-Hak, M. (1998b) A New Approach to Constrained Shape Optimization Using Genetic Algorithms, *AIAA J.* **36**, pp. 51—61.

Smits, J.G. (1990) Piezoelectric Micropump with Three Valves Working Peristaltically, *Sensors & Actuators A* **21—23**, pp. 203—206.

Taylor, G. (1972) Low-Reynolds-Number Flows, in *Illustrated Experiments in Fluid Mechanics*, pp. 47—54, National Committee for Fluid Mechanics Films, MIT Press, Cambridge, Massachusetts.

Van Lintel, H.T.G., Van de Pol, F.C.M., and Bouwstra, S. (1988) A Piezoelectric Micropump Based on Micromachining of Silicon, *Sensors & Actuators* **15**, pp. 153—167.

Von Smoluchowski, M. (1898) Ueber W rmeleitung in verd nnten Gasen, *Annalen der Physik und Chemie* **64**, pp. 101—130.

Wannier, G.H. (1950) A Contribution to the Hydrodynamics of Lubrication, *Quart. Appl. Math.* **8**, pp. 1—32.